J Neurophysiol 91: 2273–2280, 2004.
First published December 17, 2003; 10.1152/jn.00900.2003.

Equalization of Synaptic Efficacy by Activity- and Timing-Dependent Synaptic Plasticity

Clifton C. Rumsey and L. F. Abbott
Volen Center for Complex Systems and Department of Biology, Brandeis University, Waltham, Massachusetts 02454-9110

Submitted 15 September 2003; accepted in final form 11 December 2003

Rumsey, Clifton C. and L. F. Abbott. Equalization of synaptic efficacy by activity- and timing-dependent synaptic plasticity. *J Neurophysiol* 91: 2273–2280, 2004. First published December 17, 2003; 10.1152/jn.00900.2003. In many neurons, synapses increase in strength as a function of distance from the soma in a manner that appears to compensate for dendritic attenuation. This phenomenon requires a cooperative interaction between local factors that control synaptic strength, such as receptor density and vesicle release probability, and global factors that affect synaptic efficacy, such as attenuation and boosting by active membrane conductances. Anti-spike-timing-dependent plasticity, in combination with nonassociative synaptic potentiation, can accomplish this feat even though it acts locally and independently at individual synapses. Analytic computations and computer simulations show that this combination of synaptic plasticity mechanisms equalizes the efficacy of synapses over an extended dendritic cable by adjusting local synaptic strengths to compensate for global attenuation.

INTRODUCTION

The impact of an individual synapse on the firing pattern of a neuron depends not only on its intrinsic strength but also on its location in relation to the overall morphology and conductance profile of the neuron. Due to attenuation, a proximal synapse with a modest conductance can have a more powerful effect on neuronal firing than a higher-conductance synapse located distally. This greatly complicates problems associated with the development and maintenance of response selectivity. Mechanisms of synaptic plasticity have direct access to and a direct effect on local factors governing synaptic strength, such as receptor density and vesicle release probability. But to be of functional value, they should control the impact that a particular synapse has on the postsynaptic response, which depends on nonlocal factors. How do local synaptic plasticity mechanisms account and compensate for global factors, such as synaptic location, that have a powerful effect on functional synaptic efficacy?

There is growing experimental evidence that synapses on many neurons are adjusted to compensate for distance-dependent attenuation. In a number of different preparations (Alvarez et al. 1997; Andersen et al. 1980; Andrásfalvy and Magee 2001; Andrásfalvy et al. 2003; Iansek and Redman 1973; Jack et al. 1981; Korn et al. 1993; Magee and Cook 2000; Smith et al. 2003; Stricker et al. 1996; Triller et al. 1990), synapses appear to grow stronger the further out they are on the dendritic tree in such a way that somatic postsynaptic potentials are roughly equalized. Cortical layer 5 pyramidal cells appear not to follow this pattern (Williams and Stuart 2002), but this may be due to dendritic spiking mechanisms (Golding et al. 2002) or other effects (London and Segev 2001) that differentiate between in vitro and in vivo measures of synaptic efficacy. What mechanisms allow synapses to adjust their intrinsic strengths to compensate for location-dependent attenuation?

We argue here that a form of spike-timing-dependent synaptic plasticity provides a mechanism for answering these questions (for a related discussion, see Goldberg et al. 2002). Spike-timing-dependent plasticity is a form of long-term synaptic modification in which the relative timing between pre- and postsynaptic action potentials determines the magnitude and sign of long-lasting changes of synaptic strength. A variety of forms of spike-timing-dependent plasticity (STDP) have been found experimentally (reviewed in Abbott and Nelson 2000). Here, we examine the functional implications of a form referred to as anti-STDP (Goldberg et al. 2002). In conventional STDP, presynaptic spikes that occur shortly before the postsynaptic response produce long-term potentiation (LTP, Fig. 1*A*), whereas in anti-STDP, pre-before-post pairing produces long-term depression (LTD, Fig. 1*B*). We study the effects of anti-STDP in combination with a nonassociative form of LTP, a combination seen in studies of synaptic plasticity in electric fish (Bell et al. 1997; Han et al. 2000; Roberts and Bell 2000).

METHODS

The simulation results we present are based on a multicompartment model constructed using the program NEURON (Hines and Carnevale 1997). A somatic compartment containing Hodgkin-Huxley conductances was connected to a single, 50-compartment, unbranched passive cable, acting as an equivalent cable for an extended dendritic tree. The cable was one electrotonic length constant long. The cylindrical somatic section had a diameter of 20 m and a length of 20 m. The dendritic cable had a diameter of 2 m and a length of 1,000 m. The resting potential of both the soma and cable was 67.6 mV, and both had a membrane capacitance of 1 F/cm^2. The passive cable had an axial resistivity of 50 · cm and a membrane conductance of 10 ^{4} S/cm^2. The membrane time constant of the cable was thus 10 ms. Postsynaptic action potentials were generated at the somatic compartment by the standard Hodgkin-Huxley-type conductances included in the NEURON package (Hines and Carnevale 1997).

One hundred excitatory synaptic conductances with a reversal potential of zero were placed uniformly along the cable, 2 of them per cable compartment. In addition, 20 inhibitory conductances with a reversal potential of 70 mV were placed uniformly along the cable. Excitatory and inhibitory synapses were activated by presynaptic

Address reprint requests and other correspondence to: C. Rumsey (E-mail: rumsey@brandeis.edu).

The costs of publication of this article were defrayed in part by the payment of page charges. The article must therefore be hereby marked "*advertisement*" in accordance with 18 U.S.C. Section 1734 solely to indicate this fact.

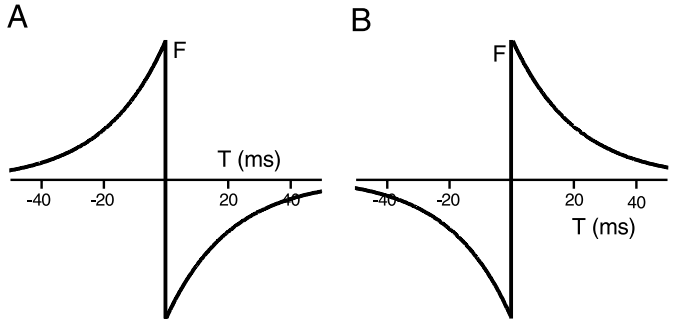

FIG. 1. Spike-timing window functions. The plotted function, $F(T)$, determines the amount and sign of changes in synaptic strength due to pre-post spike pairs separated by a time interval T. Pre-before-post ordering corresponds to T 0 and post-before-pre to T 0. The vertical scale is unspecified in these schematic diagrams because it depends on a number of factors (see METHODS for specific values). *A*: spike-timing-dependent plasticity (STDP). Pre-before-post ordering leads to long-term potentiation (LTP), and post-before-pre to long-term depression (LTD). *B*: anti-STDP. Pre-before-post ordering leads to LTD and post-before-pre to LTP.

action potentials generated by independent, random, Poisson processes with a rate constant of 10 Hz. Each presynaptic spike activated a synaptic conductance described by a difference of exponentials with rise time constants of 0.2 and 1 ms and decay time constants of 2 and 8 ms for excitatory and inhibitory synapses, respectively. The integration time step was 0.1 ms.

The maximal conductances of the inhibitory synapses were held fixed. The maximal conductances of the excitatory synapses were allowed to vary according to an anti-STDP plasticity rule combined with nonassociative potentiation. Specifically, we expressed the spike-timing window function as

$$F(T) = A \exp(T/) \quad \text{if } T \quad 0 \quad \text{and} \quad F(T) \quad 0 \quad \text{if} \quad T \quad 0 \qquad (1)$$

with A_{-} 0.01 and $_{-}$ 30 ms. No spike-timing dependent LTP was included in the simulations.

Synaptic currents were defined as $g_E w(V - E_E)$ and $g_I(V - E_I)$, respectively, with E_E 0 and E_I 70 mV. The conductance parameters g_E and g_I are given in the following text, and the factor w is the synaptic weight that is adjusted by the plasticity mechanisms we discuss. To set the scale for plasticity, synaptic weights were normalized to have an initial value of 1. The actual synaptic conductance is quantified by the excitatory postsynaptic potential (EPSP) amplitudes shown in Figs. 2 and 3. For every pair of pre- and postsynaptic action potentials, the relevant synaptic weight was augmented by $F(T)$, where T is the time difference for the given pair. In addition, nonassociative LTP was included by increasing the weight at a synapse by k 0.0024 every time a presynaptic spike occurred.

All the parameters for the "high-conductance" simulation shown in Fig. 3 were the same as those for the simulation of Fig. 2 except that the excitatory and inhibitory conductance parameters were g_E 0.28 nS and g_I 0.1 nS for Fig. 2 and g_E 0.84 nS and g_I 21 nS for Fig. 3. For the measurements of synaptic efficacy shown in Figs. 2 and 3, the pre-post cross-correlation function was determined for each synapse while all of the synapses were being activated by random, Poisson processes. Then to obtain the efficacy, the cross-correlation function was integrated, and the baseline probability was subtracted to obtain the excess pre-before-post probability.

RESULTS

Our results are presented in three forms. First, we provide a verbal description of how and why we expect anti-STDP to lead to an equalization of synaptic efficacies across an extended dendritic tree. We then back up this verbal discussion with a mathematical analysis of equations expressing in probabilistic terms how pairs of pre- and postsynaptic spikes affect synaptic strengths. Finally, we present a simulation of a multicompartmental cable model to further illustrate and explore this phenomenon.

Synaptic equalization by anti-STDP

A number of unique and useful features arise when spike-timing effects are incorporated into Hebbian synaptic plasticity. Here we make use of the ability of spike-timing plasticity mechanisms to effectively measure synaptic efficacy and use this information to guide the adjustment of synaptic strength. It is important in this discussion to distinguish between synaptic strength and synaptic efficacy. By synaptic strength, we mean the local factors, such as total receptor conductance and vesicle release probability, that can be modified directly by synaptic plasticity mechanisms. By synaptic efficacy, we mean the probability that an action potential arriving at a synaptic terminal results in the generation of a postsynaptic spike, something typically extracted from spike-train correlation functions (see for example Reid 2001).

Spike-timing-dependent forms of plasticity are sensitive to synaptic efficacy because they distinguish between presynaptic spikes that occur before and after a postsynaptic response. Synaptic efficacy is determined by measuring the probability that a presynaptic action potential is paired with a subsequent postsynaptic spike, after removing the contribution from chance occurrences of such pairs. One way of doing this is to count the number of presynaptic action potentials that occur over a short time interval prior to each postsynaptic spike and subtract from this the number of spikes occurring over a similar interval after each postsynaptic spike. Because a post-before-pre spike ordering cannot correspond to an evoked response, this procedure removes spike pairs that occur purely by chance, leaving the excess of pairs in which the presynaptic spike occurred before the postsynaptic response as a measure of the efficacy of the synapse.

Suppose for a moment that the curve in Fig. 1 was antisymmetric, that is, the LTP and LTD processes produce equal magnitude, though opposite, effects (this is the easiest case to discuss, the general asymmetric case is considered below). In this case, assuming that the effects of different spike pairs sum linearly (see DISCUSSION), the LTP and LTD processes perform a subtraction similar to that described in the preceding text. In other words, randomly occurring pre- and postsynaptic spike pairs will produce equal amounts of LTP and LTD and thus no net change in synaptic strength. However, the small excess of presynaptic spikes that evoke and therefore precede postsynaptic spikes will produce a net change of synaptic strength. Furthermore, the rate of this change will be proportional to the efficacy of the synapse because efficacy is a measure of the number of such excess pre-before-post spike pairings. In the case of STDP, synapses will increase in strength at a rate proportional to their efficacy, and in the case of anti-STDP, they will decrease in strength at a similar rate.

Our goal is to achieve an equilibrium state in which the strength of a synapse stabilizes at a level that results in a prescribed efficacy, independent of dendritic location. To do this, the ever increasing or decreasing strengths produced by STDP or anti-STDP must be compensated by another process.

In the electric fish (Bell et al. 1997; Han et al. 2000; Roberts and Bell 2000), anti-STDP is seen in combination with a nonassociative, timing-independent form of LTP, suggesting such a compensatory mechanism. A stable state with fixed efficacy (not strength) can be obtained by combining anti-STDP, which decreases synaptic strength at a rate proportional to synaptic efficacy, with nonassociative LTP, which increases synaptic strength at a rate independent of synaptic efficacy (a similar stable state cannot be obtained by using STDP). As we show in the following text through both analytic calculations and computer simulations, these two opposing processes come to equilibrium and cancel each other when a synapse achieves a specific efficacy, independent of its location. This results in an equalization of synaptic efficacy across a dendritic cable due to a distance-dependent gradient of synaptic strengths.

Mathematical analysis

The mathematical analysis we present is based on a well-established approach to calculating the effects of various patterns of pre- and postsynaptic spiking on synaptic strength through STDP (Aharonov et al. 2001; Cateau and Fukai 2003; Gütig et al. 2003; Kempter et al. 1999, 2001; Kistler and van Hemmen 2000; Rubin et al. 2001; van Rossum et al. 2000). The basic approach is to assume that changes in synaptic strength arising from multiple pre- and postsynaptic spikes add linearly (see DISCUSSION), so that the rate of change of synaptic strength for a given synapse is determined by the rate at which pre-post spike pairs separated by various intervals occur. Specifically, the effect of spike pairs separated by a particular interval is expressed as the product of the rate at which such pairs occur and a function that describes their effect on synaptic strength. The total rate of change is then calculated by integrating this product over all possible values of the pre-to-post interspike interval.

We characterize the strength of a synapse labeled by the index i by a parameter w_i, which could be a measure of total postsynaptic receptor conductance or probability of vesicle release or any combination of local factors determining synaptic strength. We use an STDP rule in which the amount of modification, w_i, of a synapse characterized by strength w_i due to a single pair of pre- and postsynaptic action potentials separated by an interval T is given by w_i $F(T)$. Here, T is the time of the presynaptic spike minus the time of the postsynaptic spike, and $F(T)$ is known as the spike-timing window function (Fig. 1). We assume that $F(T)$ depends only on the spike-timing difference T and not on the strength of the synapse (see DISCUSSION).

The calculation described in the first paragraph of this section requires two quantities. One is the spike-timing window function, $F(T)$, discussed in the preceding text. The other is the pre-post cross-correlation function, $_i(T)$, which describes the rate of occurrence of pre-post spike pairs at synapse i separated by a time interval T. In terms of these two functions, the rate of change of synaptic strength w_i for a synapse labeled by the index i is given by

$$\frac{\mathrm{d}w_i}{\mathrm{d}t} \quad \mathrm{d}TF\ T \ _i\ T \tag{2}$$

The integral in this expression sums over all possible intervals between pre- and postsynaptic action potentials. Before analyzing the consequences of this equation, we present specific features of the spike-timing window function, $F(T)$, and cross-correlation function, $_i(T)$, relevant for evaluating this integral.

Anti-STDP window function

We do not need to specify a precise form for the spike-timing window function to proceed with our analysis, but the general form we assume is shown in Fig. 1, and a specific form is given in *Eq. 1*. It is sufficient to introduce a few parameters that characterize the features of the window function relevant for our analysis. These are the total area under the spike-timing window function

$$\mathrm{d}TF\ T \tag{3}$$

and the areas under its negative and positive interval portions

$$^{0}\ \mathrm{d}TF\ T \quad \text{and} \quad \ \mathrm{d}TF\ T \tag{4}$$
^{0}

so that . Anti-STDP corresponds to the case when 0 and 0. For reasons of stability, we focus on cases when the total area is nonpositive, 0.

Cross-correlation function

In the approximation we use for our analytic calculations, the cross-correlation function has two basic components: a constant baseline correlation due to random pairings of pre- and postsynaptic action potentials and a time-dependent component the reflects evoked responses. The baseline correlation is equal to the product of the pre- and postsynaptic firing rates, defined as r_i and R, respectively. In addition, evoked responses produce an excess probability of a presynaptic spike occurring shortly before a postsynaptic spike. The magnitude of this excess above baseline is a measure of the efficacy of the synapse.

In summary, the correlation function consists of a constant term equal to r_iR, and a term corresponding to evoked responses that is proportional to $w_i^{\mathrm{eff}}r_i$, where w_i^{eff} is the efficacy of synapse i (related to, but not to be confused with, the synaptic strength w_i). The factor of presynaptic rate, r_i, in the evoked-response term is present because w_i^{eff} is defined as the efficacy per presynaptic action potential.

Evaluation of the weight-evolution equation

To evaluate the right side of *Eq. 2*, we split it into two terms corresponding to pre-before-post and post-before-pre orderings. The pre-before-post ordering receives contributions from both the background correlation and the evoked response, so we can write it as

$$^{0}\ \mathrm{d}TF\ T \ _i\ T \qquad r_i\ R \quad \frac{w_i^{\mathrm{eff}}}{^{\mathrm{eff}}} \tag{5}$$

The first term is just the area of the pre-before-post side of the spike-timing window function times the magnitude of the constant correlation. The second term is the contribution from

evoked responses, where $^{\text{eff}}$ is a time constant related to the specific time dependence of the correlation function. For example, if the correlation of pre-before-post spike pairs falls off exponentially as a function of their time difference with a time constant $_c$, $^{\text{eff}}$ $_c$. However, an exact expression for $^{\text{eff}}$ will not be needed for our analysis. In the following analysis, we assume that $^{\text{eff}}$ is a constant. This is an approximation, but we have checked its validity by examining pre-post correlation functions in multicompartmental cable model simulations. The validity of the mathematical analysis based on this assumption is also verified by the fact that the simulation results match the analytic results extremely well.

For post-before-pre spike ordering, there is no contribution from evoked responses and only the background correlation contributes, so

$$\int_0 d\tau F(\tau) C(\tau) \quad {}_i C \quad r_i R \tag{6}$$

Combining results *5* and *6, Eq. 2* becomes

$$\frac{dw_i}{dt} \quad r_i R \quad \frac{w_i^{\text{eff}} r_i}{^{\text{eff}}} \tag{7}$$

Both the postsynaptic firing rate, R, and the synaptic efficacy, w_i^{eff}, are increasing functions of the synaptic strength w_i. Therefore when 0 and 0, *Eq. 7* implies that the synaptic strength will steadily decrease over time. To compensate for this decrease, we must introduce another form of plasticity.

As mentioned in the INTRODUCTION, we investigate anti-STDP in combination with a nonassociative form of LTP that depends only on presynaptic activity. Specifically, we include a form of LTP that, by itself, would cause synaptic strengths to increase in proportion to the presynaptic firing rate, $dw_i/dt \quad kr_i$, with k a constant. If this non-Hebbian LTP is combined with the anti-STDP effects described by *Eq. 7,* we find that

$$\frac{dw_i}{dt} \quad r_i \; k \quad R \quad \frac{w_i^{\text{eff}}}{^{\text{eff}}} \tag{8}$$

where we have specialized to the case 0 and 0. This equation provides the basis for our analysis.

Antisymmetric anti-STDP and non-Hebbian LTP

For our initial analysis of *Eq. 8,* we assume that anti-STDP is antisymmetric, , so that the total area under the spike-timing window function is zero (0). We make the initial assumption of an antisymmetric window function because it simplifies the analysis somewhat. Later, we generalize to the asymmetric case when the total area is nonzero (0). In the antisymmetric case, *Eq. 8* reduces to

$$\frac{dw_i}{dt} \quad r_i \; k \quad \frac{w_i^{\text{eff}}}{^{\text{eff}}} \tag{9}$$

which has a stable fixed point when

$$w_i^{\text{eff}} \quad \frac{k \; ^{\text{eff}}}{} \tag{10}$$

Stability follows from the fact that w_i^{eff} is an increasing function of w_i. Note that *Eq. 10* implies that the synaptic efficacy is determined solely by parameters that are independent of synaptic strength and that it takes a value that is independent of i and thus the same for all synapses. This means that anti-STDP in conjunction with non-Hebbian LTP sets the efficacy of every synapse to the same value, independent of its location on the dendritic tree or any other nonlocal factors. Thus despite the fact that it only acts on synaptic strengths, anti-STDP regulates and equalizes synaptic efficacies.

Asymmetric anti-STDP and non-Hebbian LTP

The antisymmetry of the anti-STDP rule assumed in the previous section is not essential for synaptic equalization; it merely simplifies the analysis. However, it is important that LTD dominates over LTP when integrated over the entire anti-STDP spike-timing window. Thus we consider the case of negative total area under the window function, 0. The anti-STDP seen in the electric fish preparation (Bell et al. 1997; Han et al. 2000; Roberts and Bell 2000) corresponds to 0, that is, no LTP. When 0, rather than being equal to zero as in the previous analysis, *Eq. 8* has a stable fixed point (again it is straightforward to demonstrate stability provided that 0) when

$$w_i^{\text{eff}} \quad \frac{k \quad R \; ^{\text{eff}}}{} \tag{11}$$

This equation determines w_i^{eff} implicitly because the postsynaptic rate R depends on synaptic efficacy. To proceed, we must assume some form for this dependence. If we make the standard approximation that R is given by the sum of products of synaptic efficacies and presynaptic firing rates, $R \quad w_i^{\text{eff}} r_i$, *Eq. 11* can be solved easily to obtain

$$w_i^{\text{eff}} \quad \frac{k \; ^{\text{eff}}}{r_{\text{tot}} \; ^{\text{eff}}} \tag{12}$$

where $r_{\text{tot}} \quad r_i$. With these efficacies, the postsynaptic firing rate is

$$R \quad \frac{k r_{\text{tot}} \; ^{\text{eff}}}{r_{\text{tot}} \; ^{\text{eff}}} \tag{13}$$

The right side of *Eq. 12,* although slightly different from *Eq. 10,* is nevertheless independent of i. This means that all synapses are, as in the antisymmetric case, regulated to the same synaptic efficacy. Furthermore, *Eq. 13* implies that the postsynaptic firing rate is regulated by this combination of synaptic plasticities so that it is bounded, $R \quad k/$, no matter how large the presynaptic firing rates. Thus asymmetric anti-STDP in conjunction with nonassociative LTP equalizes synaptic efficacies and also regulates postsynaptic firing rates, buffering them against excessively strong total presynaptic input. Although we have assumed a simple, linear relation for the dependence of postsynaptic firing rate on synaptic efficacy, these results should generalize to any case where the postsynaptic firing rate is an increasing function of synaptic efficacy. This is verified in at least one nonlinear case by the simulations presented in the following section.

Simulation results

To further examine synaptic equalization, we constructed an equivalent cable model of a neuron known as the Rall model

(Rall 1959, 1977). The model has an active soma with Hodgkin-Huxley conductances attached to a passive dendritic cable one electrotonic length constant long. Simulation results are shown in Fig. 2. Initially, the maximal conductances for all the excitatory synapses were set to the same value (Fig. 2*A*). As seen in Fig. 2*C* (blue dots), this resulted in somatic EPSPs with amplitudes that decrease with increasing distance of the synapse from the soma, due to cable attenuation. EPSPs measured along the cable at the site of the synapse have a U-shaped profile (red dots in Fig. 2*C*) due to the decreased load of the cable at its ends where current flows in only one direction.

When the model was run for enough time so that an equilibrium configuration of synaptic strengths was established, the maximal synaptic conductances increased as a function of their distance from the soma (Fig. 2*B*). This configuration was stable and did not change, except for small random fluctuations, when the simulation was run for much longer time periods. The systematic increase in maximal synaptic conductance as a function of distance made EPSPs, measured at the site of the synapse, larger for distal than for proximal synapses (Fig. 2*D*, red dots). This increase was sufficient to cause the amplitude of EPSPs measured at the soma to be independent of distance (Fig. 2*D*, blue dots). This is in striking agreement with the data reported by Magee and Cook (2000). Note that, as in the data, there is variability in the strength from synapse to synapse, but that equalization occurs on average.

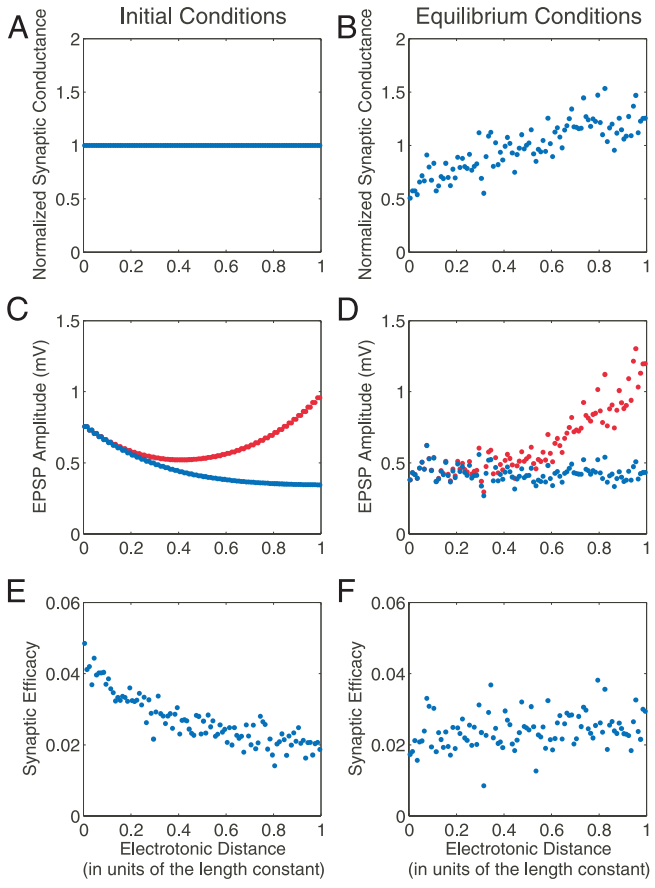

FIG. 2. Equalization of synaptic efficacies by anti-STDP in an equivalent cable model. In these plots, distance is measured in units of the electrotonic length constant of the cable, and each dot represents 1 synapse. *A*: initial, maximal excitatory synaptic conductances, normalized to their initial value and plotted as a function of the distance of the corresponding synapse from the soma. Originally all synapses have the same strength. *B*: equilibrium conductance values after equilibration of anti-STDP. Synaptic strengths increase as a function of the distance of the synapse from the soma. *C*: initial excitatory postsynaptic potential (EPSP) amplitudes. Red dots, EPSPs measured at the site of the synapse; blue dots, EPSPs measured at the soma. Amplitudes were measured by activating synapses one at a time. *D*: equilibrium dendritic and somatic EPSP amplitudes. The increase of dendritic EPSP size with distance (red dots) is sufficient to equalize EPSP sizes at the soma (blue dots). *E*: initial synaptic efficacy decreases with distance. *F*: after anti-STDP, synaptic efficacy is equalized, independent of synaptic location.

Synaptic efficacy was determined by computing the pre-post cross-correlation function for each synapse. An important difference is that whereas EPSPs were measured by activating each synapse individually, efficacies were measured while synapses all along the cable were active (see METHODS). Initially, efficacies decreased for synapses farther away from the soma (Fig. 2*E*). As Fig. 2*F* shows, however, anti-STDP acted to equalize synaptic efficacies, independent of synaptic location, as predicted by *Eq. 12*.

In a comment on the Magee and Cook (2000) paper, London and Segev (2001) pointed out that under in vivo conditions, with many synaptic conductances active simultaneously, somatic EPSPs that appeared equal in vitro, would not remain independent of synaptic location. To examine this issue, we tested the effect of using larger synaptic conductances in the model. Figure 3 shows the results of the simulation using these large synaptic conductances. As in the previous simulation, the stable equilibrium configuration of synaptic weights consists of maximal synaptic conductances that increased with increasing distance from the soma (Fig. 3*B*). However, the conductances increased to a greater degree. This resulted in larger local dendritic EPSPs (Fig. 3*D*, red dots), and, notably, somatic EPSP amplitudes that were not equalized as they were when synaptic conductances were small (Figs. 3*D* vs. 2*D*, blue dots).

Even though equilibrium somatic EPSPs increased with increasing distance under high-conductance conditions (Fig. 3*D*, blue dots), the equalization effect of anti-STDP on synaptic efficacies remained (Fig. 3*F*). This shows that anti-STDP equalizes synaptic efficacies not somatic EPSPs. When the synaptic conductances are sufficiently low, equalizing efficacies leads to the equalization of EPSPs. When synaptic conductances are high, efficacies and EPSP amplitudes differ because EPSPs are measured through activation of individual synapses (in vitro conditions), whereas efficacies are measured under in vivo conditions with simultaneous activation of many synapses. Although true equalization of somatic EPSPs fails in the example of Fig. 3, equalization applies quite well if the synapses are not too far out on the dendrite (less than 0.5 length constants). This may explain why equalization is seen experimentally even for neurons that are likely to receive a large amount of synaptic input in vivo (Magee and Cook 2000).

DISCUSSION

Standard STDP, in which pre-before-post spike ordering leads to LTP and the reverse to LTD, is a typical Hebbian process in which synapses with high efficacy tend to get stronger and synapses with low efficacy tend to get weaker. This is useful when it comes to identifying and strengthening correlated or structured inputs, but it can also lead to problems. For example, if all synapses start off with the same intrinsic

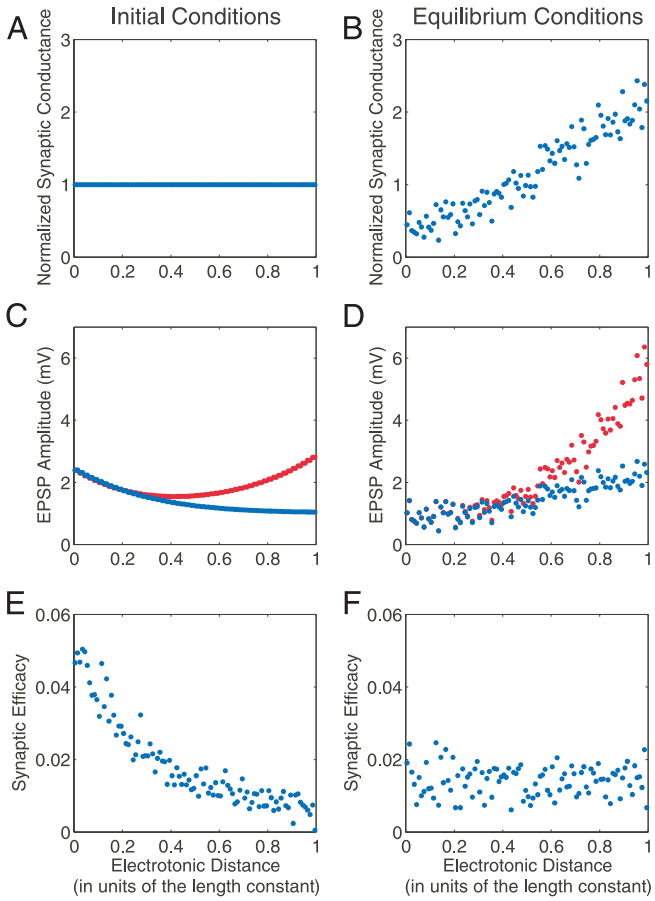

FIG. 3. Equalization of synaptic efficacies by anti-STDP in an equivalent cable model with large synaptic conductances. *A*: initial, maximal excitatory synaptic conductances. *B*: equilibrium conductances cover a much wider range than the lower conductance case of Fig. 2*B*. *C*: initial dendritic (red dots) and somatic (blue dots) EPSP amplitudes. Note that EPSP amplitudes are roughly 3 times larger than in Fig. 2*C*. *D*: equilibrium EPSP amplitudes. Somatic EPSP size (blue dots) increases with distance from the soma because of the larger local dendritic EPSPs (red dots). *E*: initial synaptic efficacy decreases with distance. *F*: equilibrium synaptic efficacy is equalized by anti-STDP, even though the somatic EPSPs are not equalized (*D*).

strength, STDP tends to strengthen proximal synapses and weaken distal synapses simply because proximal synapses are more effective at generating postsynaptic action potentials than distal ones. Similarly, groups of synapses that can generate local dendritic action potentials tend to be strengthened (Goldberg et al. 2002). Strengthening synapses on the basis of morphology and synaptic placement is not likely to be an optimal strategy for a neuron to develop useful forms of selectivity. Thus although STDP is a useful process for the development of neuronal selectivity (see, for example, Song and Abbott 2001), it can be problematic if applied in the absence of homeostatic and regulatory mechanisms.

As suggested previously by Goldberg et al. (2002), anti-STDP can provide such a regulatory mechanism. We have shown that when combined with a nonassociative form of LTP, anti-STDP can equalize synaptic efficacies, setting the stage for processes such as STDP to develop neuronal selectivity without unwanted biases due to synaptic location. We suggest that anti-STDP and nonassociative LTP act either during development or continuously, even in the adult, but at a slower rate than STDP. Thus STDP may modify synapses rapidly in response to appropriate forms of activity and reward, while anti-STDP acts more slowly as a developmental mechanism and for continuous homeostatic maintenance.

Even if STDP and anti-STDP act on different time scales, they oppose each other and tend to undo each other's effects. This problem is alleviated considerably if STDP and anti-STDP act at different loci. There is considerable evidence that STDP is at least partially, and perhaps predominantly, expressed presynaptically (Markram and Tsodyks 1996; Senn et al. 2001; Sjöström et al. 2003). If anti-STDP is expressed postsynaptically, the somewhat contradictory requirements of homeostasis and adaptation might be reconciled, with anti-STDP removing biases due to synaptic location and STDP strengthening correlated sets of inputs.

The results of this paper are based on the assumption that the effects of individual spike pairs through anti-STDP add linearly. If we use STDP as a guide, this assumption seems to hold quite well for firing rates below 30 Hz (G. Bi, private communication), but nonlinear effects appear at higher rates (Froemke and Dan 2002; Senn et al. 2001; Sjöström et al. 2001). Because average firing rates in cortical circuits tend to be 30 Hz and anti-STDP is assumed to be a relatively slow-acting process, we feel the assumption of linear summation is justified.

Equalization of synaptic efficacy by anti-STDP is robust to changes of parameters. Modifying parameters such as the rate for non-Hebbian LTP (k), or the area parameters for the anti-STDP window function (, and) changes the value that the synaptic efficacies take but does not change the fact that they are equalized. However, it should be noted that we have assumed, in this analysis, that the somatic action potential backpropagates along the dendrite sufficiently to allow the plasticity mechanism within each synapse to sense its occurance. Failure of action potential backpropagation could interfere with synaptic equalization, although this problem could be somewhat mitigated by distal dendritic spike initiation regions. These effects are currently under investigation.

A number of authors have considered spike-timing window functions that have an additional dependence on synaptic strength that we have not considered (Aharonov et al. 2001; Gütig et al. 2003; Kempter et al. 1999, 2001; Kistler and van Hemmen 2000; Rubin et al. 2001; van Rossum et al. 2000). The effect that this additional feature has on our results depends on how the synaptic strength enters into the window function. If the LTP and LTD sides of the window function have the same dependence on synaptic strength, our results are unaffected. We call this the homogeneous case. If, however, the dependence of LTP on synaptic strength is different from the dependence on LTD (the inhomogeneous case), synaptic equalization can be lost. This is because the equilibrium condition in inhomogeneous models tends to determine a specific value of synaptic strength not efficacy. We must therefore assume that anti-STDP has evolved to have a homogeneous dependence on synaptic strength, so that the resulting advantages, sensitivity to efficacy not merely strength, can be realized.

Although we have simulated synaptic equalization by anti-STDP in a passive model, our analytic results make it clear that the equalization of synaptic efficacy will occur in the presence of active conductances as well. For example, if a particular neuron has a distal dendritic spike-initiation zone (Golding et

al. 2002), we would not expect synapses near that area to be strengthened by anti-STDP as they would in a passive model. This is because such synapses will be effective at generating postsynaptic action potentials even if they produce relatively small somatic EPSPs in the absence of dendritic spiking. Nevertheless, this should be checked in multicompartment models with realistic morphology and active dendritic conductances, work that is currently in progress.

The combination of spike-timing-dependent and nonassociative forms of plasticity that we have studied is not unique in its ability to equalize synaptic efficacies, but this combination has some distinct advantages. Through its timing dependence, anti-STDP is sensitive to the efficacy of individual synapses not merely overall efficacy as would be the case for a general anti-Hebbian form of plasticity. The firing-rate dependence of the nonassociative LTP we considered assures that synapses are equalized independent of their presynaptic firing rates. Although other forms of plasticity might produce an equalization effect, they are unlikely to have these advantages.

It might be argued that a neuron could establish a gradient of synaptic strengths using structural cues rather than an activity-dependent process as we have assumed. However, recent work by Andrásfalvy, Smith, Borchardt, Sprengel, and Magee (2003) indicates that equalization of synaptic efficacy is impaired in GluR1 knockout animals. This supports the idea that synaptic transmission and activity-dependent plasticity play an important role in the equalization process.

Equalizing synaptic efficacy through an activity-dependent, rather than morphologically dependent, process has a number of advantages. Synaptic efficacy depends on so many global factors, including the distributions and densities of active membrane channels, that an activity-independent process might have difficulty compensating for all of them. Within the ranges that synaptic strength can be modified, the mechanism we propose will equalize efficacies no matter what morphological or physiological processes modify synaptic efficacy between the site of the synapses and the locus of action potential generation.

It must be acknowledged that anti-STDP has not been seen in experiments involving hippocampal or cortical neurons. One reason for this may be that it does not exist, and the analysis we have provided is academic for these systems. However, if anti-STDP acts over long time scales, only during certain periods of development, or only under certain modulatory conditions, it could well have been missed. Given its ability to perform a highly useful regulatory task, the equalization of synaptic efficacies, we argue for its existence and suggest that it should be looked for.

ACKNOWLEDGMENTS

We are extremely grateful to R. Gütig for the insights shared during this project and to H. Sompolinksy for comments and suggestions.

GRANTS

This research was supported by the National Institutes of Health Grants MH-58754 and NS-047054-01 to C. Rumsey.

REFERENCES

Abbott LF and Nelson SB. Synaptic plasticity: taming the beast. *Nat Neurosci* 3: 1178–1183, 2000.

Aharonov R, Gütig R, Rotter S, Aertsen A, and Sompolinsky H. Generalized synaptic updating in temporally asymmetric Hebbian learning. In: *Computational Neuroscience, Trends in Research 2001*, edited by Bower J. Amsterdam: Elsevier, 2001.

Alvarez FJ, Dewey DE, Harrington DA, and Fyffe RE. Cell-type specific organization of glycine receptor clusters in the mammalian spinal cord. *J Comp Neurol* 379: 150–170, 1997.

Andersen P, Silfvenius H, Sundberg SH, and Sveen O. A comparison of distal and proximal dendritic synapses on CA1 pyramids in guinea pig hippocampal slices in vitro. *J Physiol* 307: 273–299, 1980.

Andrásfalvy BK and Magee JC. Distance-dependent increase in AMPA receptor number in the dendrites of adult hippocampal CA1 pyramidal neurons. *J Neurosci* 21: 9151–9159, 2001.

Andrásfalvy BK, Smith MA, Borchardt T, Sprengel R, and Magee JC. Impaired regulation of synaptic strength in hippocampal neurons from GluR1-deficient mice. *J Physiol* 552: 35–45, 2003.

Bell CC, Han VZ, Sugawara Y, and Grant K. Synaptic plasticity in a cerebellum-like structure depends on temporal order. *Nature* 387: 278–281, 1997.

Cateau H and Fukai T. A stochastic method to predict the consequence of arbitrary forms of spike-timing-dependent plasticity. *Neural Comput* 15: 597–620, 2003.

Froemke RC and Dan Y. Spike-timing-dependent synaptic modification induced by natural spike trains. *Nature* 416: 433–438, 2002.

Goldberg J, Holthoff K, and Yuste R. A problem with Hebb and local spikes. *Trends Neurosci* 25: 433–435, 2002.

Golding NL, Staff NP, and Spruston N. Dendritic spikes as a mechanism for cooperative long-term potentiation. *Nature* 18: 326–331, 2002.

Gütig R, Aharonov R, Rotter S, and Sompolinksky H. Learning input correlations through nonlinear temporally asymmetric Hebbian plasticity. *J Neurosci* 23: 3697–3714, 2003.

Han VZ, Grant K, and Bell CC. Reversible associative depression and nonassociative potentiation at a parallel fiber synapse. *Neuron* 27: 611–622, 2000.

Hines ML and Carnevale NT. The NEURON simulation environment. *Neural Comput* 9: 1179–1209, 1997.

Iansek R and Redman SJ. The amplitude, time course and charge of unitary post-synaptic potentials evoked in spinal motoneuron dendrites. *J Physiol* 234: 665–688, 1973.

Jack JJB, Redman SJ, and Wong K. The components of synaptic potentials evoked in cat spinal motoneurons by impulses in single group Ia afferents. *J Physiol* 321: 65–96, 1981.

Kempter R, Gerstner W, and van Hemmen JL. Hebbian learning and spiking neurons. *Phys Rev E* 59: 4498–4514, 1999.

Kempter R, Gerstner W, and van Hemmen JL. Intrinsic stabilization of output rates by spike-based Hebbian learning. *Neural Comput* 13: 2709–2741, 2001.

Kistler WM and van Hemmen JL. Modeling synaptic plasticity in conjunction with the timing of pre- and postsynaptic action potentials. *Neural Comput* 12: 385–405, 2000.

Korn H, Bausela F, Charpier S, and Faber DS. Synaptic noise and multiquantal release at dendritic synapses. *J Neurophysiol* 70: 1249–1254, 1993.

London M and Segev I. Synaptic scaling in vitro and in vivo. *Nat Neurosci* 4: 853–855, 2001.

Magee JC and Cook EP. Somatic EPSP amplitude is independent of synapse location in hippocampal pyramidal neurons. *Nat Neurosci* 3: 895–903, 2000.

Markram H and Tsodyks M. Redistribution of synaptic efficacy between neocortical pyramidal neurons. *Nature* 382: 807–810, 1996.

Rall W. Branching dendritic trees and motoneuron membrane resistivity. *Exp Neurol* 1: 491–527, 1959.

Rall W. Core conductor theory and cable properties of neurons. In: *Handbook of Physiology. The Nervous System: Cellular Biology of Neurons*. Bethesda, MD: Am. Physiol. Soc., 1977, sect. 1, vol. 1, pt. 1, p. 39–97.

Reid RC. Divergence and reconvergence: multielectrode analysis of feedforward connections in the visual system. *Prog Brain Res* 130: 141–154, 2001.

Roberts PD and Bell CC. Computational consequences of temporally asymmetric learning rules. II. Sensory image cancellation. *J Comput Neurosci* 9: 67–83, 2000.

Rubin J, Lee DD, and Sompolinksy H. Equilibrium properties of temporally asymmetric Hebbian plasticity. *Phys Rev Lett* 86: 364–367, 2001.

Senn W, Markram H, and Tsodyks M. An algorithm for modifying neurotransmitter release probability based on pre- and postsynaptic spike timing. *Neural Comput* 13: 35–67, 2001.

Sjöström PJ, Turrigiano GG, and Nelson SB. Rate, timing, and cooperativity jointly determine cortical synaptic plasticity. *Neuron* 32: 1149–1164, 2001.

Sjöström PJ, Turrigiano GG, and Nelson SB. Neocortical LTD via coincident activation of presynaptic NMDA and cannabinoid receptors. *Neuron* 39: 641–654, 2003.

Smith MA, Ellis-Davies GCR, and Magee JC. Mechanism of the distance-dependent scaling of Schaffer collateral synapses in rat CA1 pyramidal neurons. *J Physiol* 548: 245–258, 2003.

Song S and Abbott LF. Cortical development and remapping through spike-timing dependent plasticity. *Neuron* 32: 339–350, 2001.

Stricker C, Field AC, and Redman SJ. Statistical analysis of amplitude fluctuations in EPSCs evoked in rat CA1 pyramidal neurons in vitro. *J Physiol* 490: 419–441, 1996.

Triller A, Seitanidou T, Franksson O, and Korn H. Size and shape of glycine receptor clusters in a central neuron exhibit a somato-dendritic gradient. *New Biol* 2: 637–641, 1990.

van Rossum MC, Bi GQ, and Turrigiano GG. Stable Hebbian learning from spike timing-dependent plasticity. *J Neurosci* 20: 8812–8821, 2000.

Williams SR and Stuart GJ. Dependence of EPSP efficacy on synapse location in neocortical pyramidal neurons. *Science* 295: 1907–1910, 2002.